World Journal of Dental Excellence, 2025, JUNE, Vol. 1 No. 1 (2025): 59-64.

REVIEW ARTICLE

World Journal of Dental Excellence

Revolutionizing Oral Cancer Detection: Fusing The Power of Light and AI for Early Diagnosis

Darshana SN[1] | Anjani Sravya M[2] | Ramnarayan BK[3] | Mahesh DR[4] | Preeti Patil[5]

[1]Senior Lecturer, Department of Oral Medicine and Radiology, Dayananda Sagar College of Dental Sciences, Karnataka, India

[2]Under Graduate Student, Dayananda Sagar College of Dental Sciences, Karnataka, India

[3]Professor and Head of Department of Oral Medicine and Radiology, Dayananda Sagar College of Dental Sciences, Karnataka, India

[4]Reader, Department of Oral Medicine and Radiology, Dayananda Sagar College of Dental Sciences, Karnataka, India

[5]Reader, Department of Oral Medicine and Radiology, Dayananda Sagar College of Dental Sciences, Karnataka, India

Correspondence

Corresponding author: Darshana SN

Email: darshananayak@dscds.edu.in

Present address

Dayananda Sagar College of Dental Sciences, Shavige Malleshwara Hills, Kumaraswamy Layout, Bangalore 560 078, Karnataka, India

Abstract

Early detection and accurate diagnosis of oral cancer are critical for improving patient prognosis. However, current screening methods often fail to identify all lesions, highlighting the need for more effective approaches. Optical Coherence Tomography (OCT), an advanced optical imaging technology, shows promise in detecting malignant cells. OCT images require specialized interpretation due to their detailed information. Artificial Intelligence (AI), leveraging trained algorithms, can analyze imperceptible variations, overcoming barriers that have delayed OCT integration into oral cancer screening. This review explores OCT's depiction of precancerous and cancerous oral lesions and discusses AI's role in enhancing detection and diagnosis.

KEYWORDS

Oral Cancer, Early Diagnosis, Optical Coherence Tomography (OCT), Artificial Intelligence (AI), Cancer Detection

1 | INTRODUCTION

Globally, Oral Cancer ranks sixth in cancer incidence, presenting significant health challenges.[1] Oral squamous cell carcinoma (OSCC), the predominant type, emphasizes the critical importance of early detection for effective treatment and improved survival rates.[2,3] Optical Coherence Tomography (OCT) is an advanced, noninvasive imaging technique utilizing interferometry to produce high-resolution images.[4] Its rapid, three-dimensional imaging capabilities have made it increasingly valuable in various medical specialties, including oncology.[5] Artificial Intelligence (AI) has shown remarkable accuracy in biomedical imaging, aiding in personalized cancer treatment decisions.[3] The integration of AI into oral cancer research and clinical practice holds promise for improving patient outcomes.[6] AI, a field of computer science simulating human intelligence in machines, employs Machine Learning (ML) and Deep Learning (DL) techniques to analyze complex datasets and enhance diagnostic accuracy.[7]

2 | MECHANISM OF OCT

OCT uses light sources to penetrate tissues, interacting based on tissue properties such as absorption and reflection.[1] Unlike ultrasonography, OCT offers higher resolution and different receiving mechanisms, facilitating detailed imaging.[7] Interferometry is fundamental to OCT, involving the division of light into reference and sample beams to create interference patterns.[1] This principle enables OCT to capture intricate structural details from tissues, crucial for precise clinical imaging. By combining the imaging capabilities of OCT with the analytical power of AI, researchers aim to innovate oral cancer detection, potentially improving screening accuracy and patient outcomes. (Fig1)

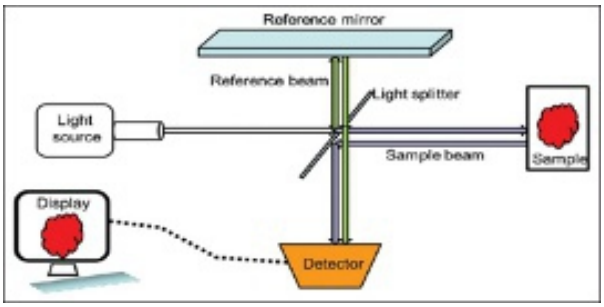

Fig:1 Basic Principle of OCT[1]

2.1 | TYPES OF OCT DEVICES

Optical Coherence Tomography (OCT) devices are classified based on their reference arm optics into time-domain and frequency-domain variants. Among frequency domain devices, two main types are spectral OCT (SD-OCT) and swept-source OCT (SS-OCT). SS-OCT employs an ultrahigh-speed laser beam with a wavelength in the kilohertz range and a center wavelength of 1300 nm. This configuration enhances system sensitivity, penetration depth, resolution, and scanning speed (achieving imaging in one second or less), thereby reducing acquisition time. The axial and transverse resolutions of SS-OCT are determined by the focal spot size and the width of the laser beam line, respectively [7]

Time-domain OCT (TD-OCT) involves measuring optical path lengths (OPLs) by moving a reference reflector, while spectral domain OCT (SD-OCT) or Fourier domain OCT (FD-OCT) calculates OPLs using various wavelengths without requiring a moving reflection mirror. An SD-OCT system shares similar components with TD-OCT but includes additional elements like a grating, sensor array (typically a CC-array), or spectrometer.[8]

Normal Mucosa in OCT: A study conducted by Albrecht, et al. in 2020 on healthy human oral mucosa in OCT image.[9]

1. Labial and Alveolar Mucosa: The epithelial surface of the alveolar mucosa was found to be intact in 92.2% and 95.4% of measurements, with a homogeneous layer observed in 96.6% and an average thickness of 142 ± 15 µm. [9]

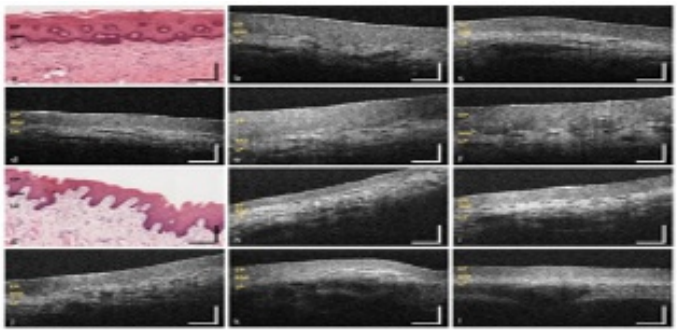

Fig:2

Optical coherence tomography (OCT) images show (b–f) the labial mucosa and (h–l) the alveolar mucosa. Representative images include the upper lip (MP1) (b, c), lower lip (MP3, MP4) (d–f), upper alveolar region (MP2) (h, i), and lower alveolar region (MP5) (j–l). Histological cross sections stained with hematoxylin and eosin (HE) depict the labial and alveolar mucosa (a, g) with modifications noted (EP: epithelium, BM: basement membrane, LP: lamina propria. Scale bars: 200 µm)."(Fig.2)

2.Buccal Mucosa: Analysis of OCT images of the buccal mucosa showed surface alterations in 30.6% of cross-sections, a homogeneous epithelium in 74.6%, and an intact basement membrane in 60.8%. Vascular supply appeared moderate in 67.7%, but additional features were not discernible due to the presence of fat tissue and limitations in imaging depth. [9]

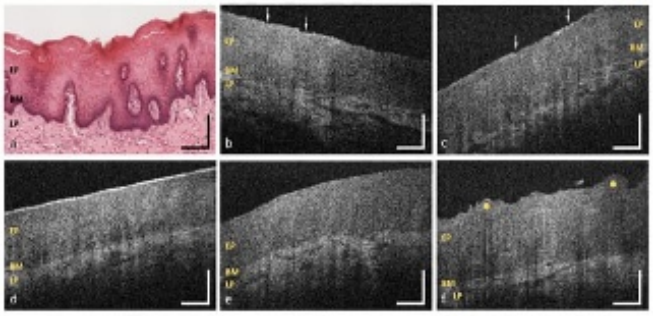

Fig: 3

CT images of the buccal mucosa are shown in (b–f). These images depict the (b, c) anterior (MP6), (d) central (MP7), and (e, f) posterior buccal regions (MP8). Histological cross sections stained with hematoxylin and eosin (HE) illustrate the buccal mucosa, highlighting key structures such as the epithelium (EP), basement membrane (BM), and lamina propria (LP). Arrows indicate areas of epithelial surface alteration, while yellow dots represent uneven surface profiles. Scale bars: 200µm(Fig.3)

3.Sublingual Mucosa: OCT images from the ventral tongue and mouth floor showed intact epithelial surfaces, homogeneous structures, and extensive vascular supply due to large sublingual arteries and veins. 86.6% of sections were highly vascularized. [9]

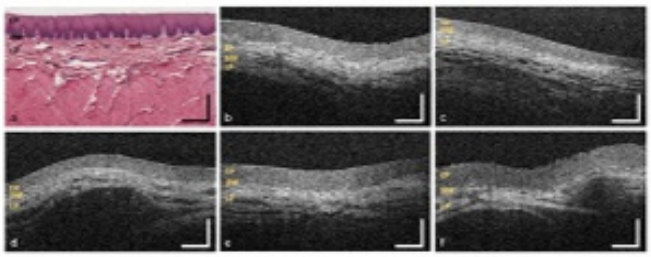

Fig: 4

OCT images of the ventral tongue (b,c) and the mouth floor (MP11) (d–f). The sample pictures represent the anterior (MP9) (b) and posterior sublingual region (MP10) (c). Exemplary HE stained histological cross sections depicting the sublingual mucosa (a). (EP: epithelium, BM: basement membrane, LP: lamina propria. Scale bars: 200 µm).(Fig.4)

4.Hard Palate: The hard palate shows various alterations in the epithelial surface, with convex ridges (38.8%) corresponding to transverse palatal folds. Approximately 37.5% of the epithelial layer exhibits inhomogeneity, reflecting adaptation to masticatory function. Female volunteers tend to exhibit lower values compared to males. The basement membrane appears indistinct, and minor salivary glands are observed in 15.0% of OCT cross-sections. [9]

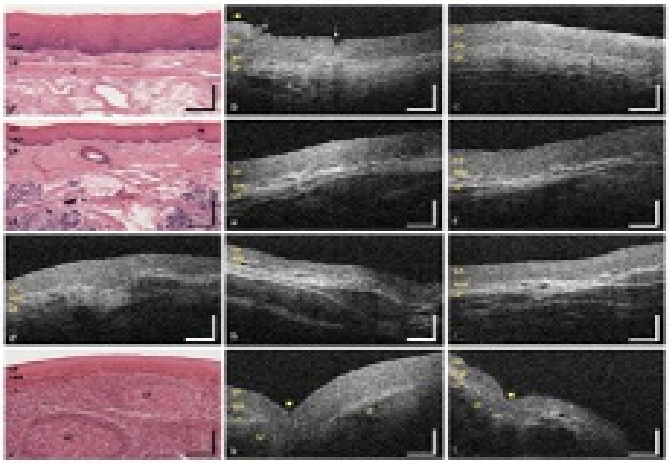

Fig:5

OCT images depict the (b, c) hard palate (MP12), (e, f) soft palate (MP13), (g) uvula (MP14), (h, i) oropharynx (MP15), and (k, l) palatine tonsil (MP16). Histological cross-sections stained with hematoxylin and eosin (HE) illustrate the (a) hard palate, (d) soft palate, and (j) palatine tonsil. Key features such as the epithelium (EP), basement membrane (BM), lamina propria (LP), and lymphoid follicle (LF) are identified. Arrows indicate areas of epithelial alteration, while yellow dots represent palatal ridges and tonsillar crypts. Scale bars: 200 µm.(fig.5)

5. Soft Palate and Oropharynx: The soft palate, uvula, and oropharynx were evaluated for the integrity of their epithelial surface, revealing a consistently homogeneous epithelium. Significant vascularization by major vessels was observed in the majority of cases (56.1%), accompanied by a well-defined vessel network within the lamina propria. Clusters of salivary glands were identified in 47.4% of cases, indicating effective moistening of the alveolar region. [9]

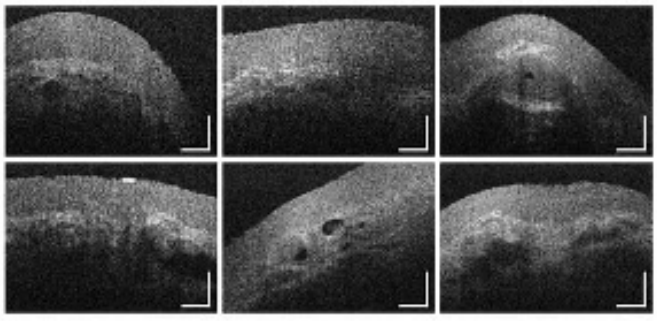

Fig:6

Additional intensity-based OCT cross-sections of the mucosal tissue were obtained for the soft palate (MP13) and the oropharynx (MP15). Scale bars: 200 µm (Fig.6)

6.Palatine Tonsils: OCT cross sections were used to analyze the palatine tonsil, revealing an intact epithelium in 70.6% of cases and an uneven surface profile in 87.5%. Age-related variations were noted, with reduced thickness observed in participants aged 25-45. The basement membrane appeared indistinct in 52.2% of cases, while moderate vascularization was evident in

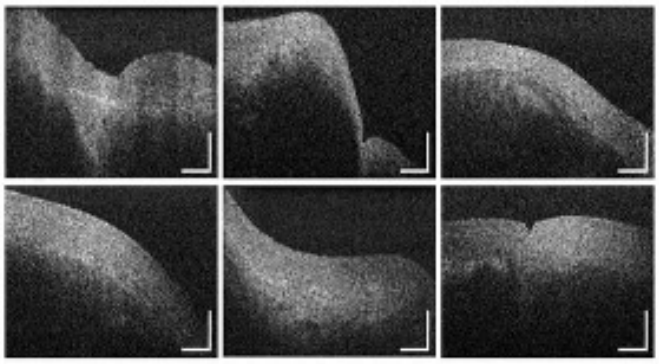

Fig: 7

Additional intensity-based OCT cross sections of the mucosal tissue from the palatine tonsil (MP16) were included. Scale bars: 200 µm.(Fig.7)

Cancer Indicators

Optical Coherence Tomography (OCT) images are capable of detecting neoplastic alterations in epithelial tissues characterized by abnormal cells with enlarged nuclei. Key histological indicators of malignancy include enlarged dysplastic cells, irregular stratification, basal hyperplasia, and elongated papilla cores. Dysplastic cells typically exhibit a scattered speckle pattern on OCT B-scans. Researchers have explored markers within the subepithelial tissue, basement membrane, and epithelial mucosa to differentiate between normal, premalignant, and cancerous tissues of the oral mucosa. Thickening of the basement membrane serves as an indication of tumor invasion, suggesting potential malignant changes. Both basement membrane integrity and epithelial thickness serve as reliable markers for distinguishing between invasive cancer and normal or dysplastic tissues. Dysplastic transformations may involve fibroblast proliferation, alterations in collagen and other extracellular components, and changes in the stromal environment. [7]

OCT images of Various lesions

1. Adenoid cystic Carcinoma:

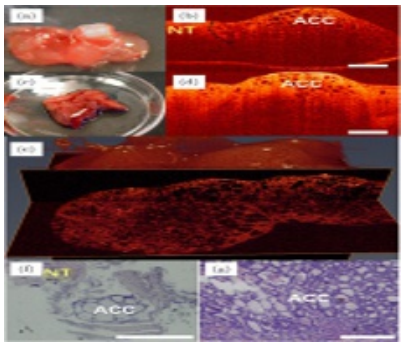

Fig: 8

Images of adenoid cystic carcinoma are presented as follows: (a) and (c) depict photographs of the specimen, while (b) and (d) show 2D OCT images of adenoid cystic carcinoma in palate tissue from two different patients. Additionally, (e) displays a 3D OCT image of adenoid cystic carcinoma. Corresponding histopathological images are provided in (f) and (g). ACC refers to adenoid cystic carcinoma, and NT indicates normal tissue.(Fig.8)[10]

2. Squamous Cell Carcinoma:

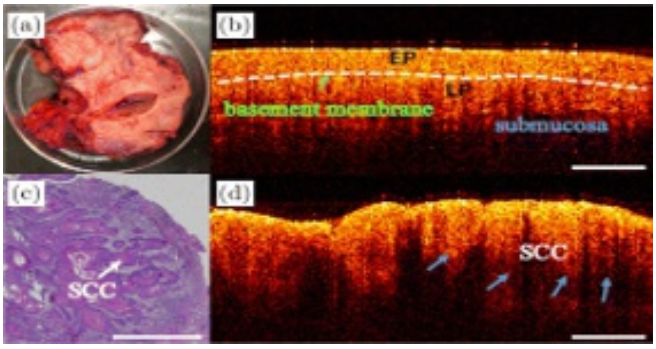

Fig: 9

Furthermore, OCT images and corresponding histology of squamous cell carcinoma (SCC) are shown: (a) is a photo of the excised tissue specimen; (b) and (d) represent 2D OCT images from different positions of the same specimen, with (b) showing normal oral mucosa and (d) showing SCC. (c) presents the corresponding histopathological image of SCC. EP denotes the epithelial layer, and LP stands for lamina propria.(fig.9) [10]

3. Basal-Cell Carcinoma:

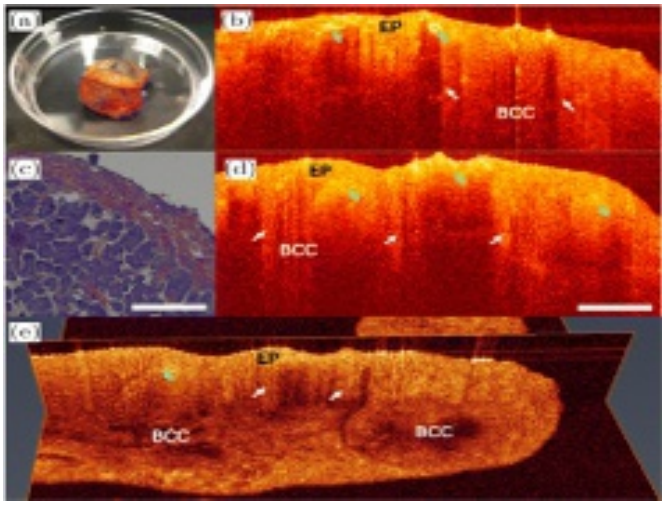

Fig: 10

Images of basal cell carcinoma (BCC) are presented as follows: Panel (a) shows a photograph of the excised tissue specimen, while panels (b) and (d) display 2D OCT images of BCC from the same patient. Panel (c) presents the corresponding histopathological image, and panel (e) shows the 3D OCT image. EP refers to epithelial tissue.(Fig.10) [10]

4. Lipoma: Images of lipoma include panel (a) featuring a photograph of the excised tissue specimen. Panel (b) shows an OCT image of the lipoma, and panel (c) depicts its corresponding histopathological image. FT denotes fibrous tissue, and FV represents fat vesicle.

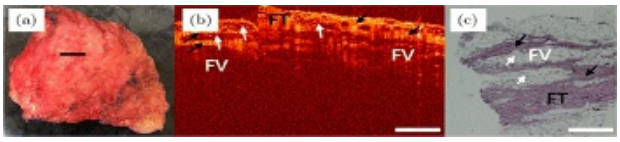

Fig: 11

Images of lipoma include panel (a) featuring a photograph of the excised tissue specimen. Panel (b) shows an OCT image of the lipoma, and panel (c) depicts its corresponding histopathological image. FT denotes fibrous tissue, and FV represents fat vesicle.(Fig.11) [10]

5. Fibrous Epulis:

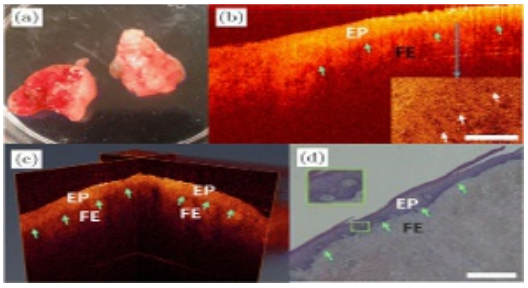

Fig: 12

For images of fibrous epulis, panel (a) shows a photograph of the excised tissue specimen. Panel (b) displays a 2D OCT image and an en-face OCT image derived from the dashed line of the fibrous epulis. Panel (c) illustrates the 3D OCT image of fibrous epulis, and panel (d) presents its histological image. EP denotes epithelial tissue, and FE stands for fibrous epulis.(Fig.12) [10]

6.Leukoplakia:

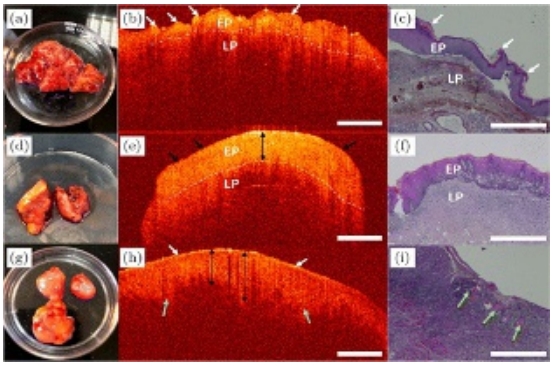

Fig: 13

OCT images and their corresponding histopathological images of leukoplakia are presented as follows: Images (a) and (d) depict photographs of tissue samples, while Images (b) and (e) show 2D OCT images of leukoplakia from two different patients. Image (g) is a photograph and (h) is a 2D OCT image showing leukoplakia with signs of canceration. Histopathological images corresponding to (a), (d), and (g) are shown in (c), (f), and (i), respectively. EP denotes the epithelial layer, and LP stands for lamina propria(Fig.13) [10]

7. Normal mucosa, Oral squamous cell carcinoma:

Morphological characteristics and statistical analysis of oral tissues are illustrated as follows: Panel (a) displays an OCT image of normal mucosa, while panels (b) and (c) show OCT images of leukoplakia with epithelial hyperplasia (LEH) and oral squamous cell carcinoma (OSCC), respectively. Corresponding histopathological images are shown in panels (d) to (f). The region of interest is indicated as 256 × 256 pixels.(Fig.14) [10]

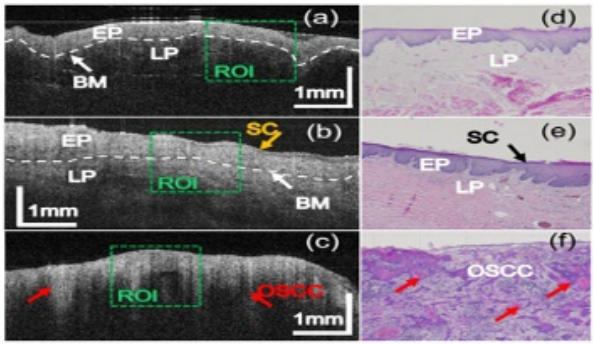

Fig: 14

Integration of AI and OCT

The use of OCT in oncology faces limitations such as restricted penetration depth, scan volume, high resolution, noise, and challenges in image interpretation, which is often operator-

Stages in Integrating OCT with AI:

1. Data collection
2. Image processing
3. Development of AI models
4. Validation of AI Models [11]

Artificial Neural Networks (ANNs) are machine learning algorithms consisting of layers of neurons, with convolutional neural networks (CNNs) being widely used for visual data analysis. These networks are trained using structured data to continuously enhance their performance.

Research employing various AI algorithms for interpreting OCT images is detailed below

1.Pande P, Shrestha S, Park J, et al. [12] (2014): The objective of this study is to assess the feasibility of using image analysis algorithms for automated characterization and classification of OCT images in a hamster cheek pouch tumour model. Additionally, the study aims to evaluate the potential of OCT-based automated diagnosis of oral cancer.

Two algorithms were used:

Algorithm 1- Algorithm for filtering A-lines in a B-scan

Algorithm 2- Algorithm for generating a binary mask corresponding to the epithelial region in a nonlayered B-scan.

The study presents a segmentation algorithm for identifying epithelial regions in OCT B-scans, achieving 80.6% sensitivity and classification accuracy, using random forest for robustness against noisy labels and overfitting.

2.Hwang DK et al.[11] (2020): OCT macula cross-section scanning images from patients with diabetic macular edema (DME) to classify the disease.

AI models were developed using GGG16 and InceptionV3, with transfer learning applied. The accuracy, sensitivity, and specificity of the models were 92.82%, 93.09%, 96.48%, 95.15%, and 89.63%, respectively.

3.James et al.[13] (2021): The aim of this study is to develop a decision tree using an OCT diagnostic system to accurately identify and differentiate between cancer/dysplastic lesions and non-dysplastic lesions in oral cancer screening. A MATLAB based simple algorithm-score and an Artificial Neural Network-Support Vector Machine (ANN-SVM) based model was used.

The study uses a retrained convolutional neural network to classify three-dimensional OCT images of head and neck mucosa, identifying normal and abnormal tissues with 100% sensitivity and 70% specificity. The algorithm predicts the severity of oral squamous cell carcinoma (OSCC) lesions based on 172 oral sub-sites. The scores for dysplastic lesions differ significantly, with sensitivity of 93% and specificity of 74%.

4. Wei Yuan et.l[14] (2022): The aim of this study was to develop the automatic non-invasive OSCC diagnosis approach to identify the malignant tissues on Optical Coherence Tomography (OCT) images.

This study used Multi-Level Deep Residual Learning (MDRL) network. The MDRL system attains the outstanding diagnostic performance, with 91.2% sensitivity, 83.6% specificity, 87.5% accuracy, 85.3% PPV, and 90.2% NPV in image-level, with 0.92 AU value. Besides, it also implements 100% sensitivity, 86.7% specificity, 93.1% accuracy, 87.5% PPV, and 100% NPV in the resected patch-level.

5. Yang et al.[10] 2020:To assess deep-learning-based algorithms for OCT images to assist clinicians in oral cancer screening and diagnosis

Three CNNs (convolutional neural networks), including LeNet-5, VGG16, and ResNet18, and Machine learning. CNNs outperform machine-learning in detecting and diagnosing oral cancer, with accuracy of 92.52% and classification accuracy of up to 96.76%, demonstrating their logic and interpretability in OCT images.

OCT images of Oral lesions interpreted by AI:

1. Oral Squamous Cell Carcinoma

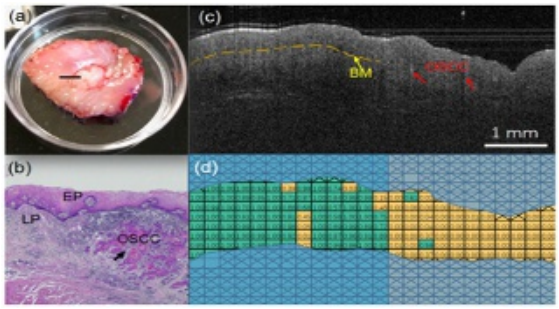

Fig: 15: a) displays an image of the excised tissue specimen. (b) presents a histopathological image where the normal region is on the left and the cancerous region is on the right. (c) shows the OCT image corresponding to (a). (d) depicts the prediction visualization of oral squamous cell carcinoma (OSCC).[2]

2. Normal mucosa, Oral squamous cell carcinoma

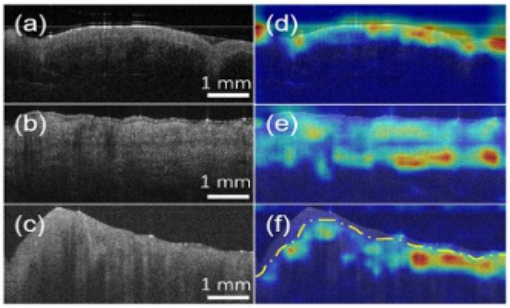

Fig: 16: Grad-CAM visualization on OCT images of oral tissues is described as follows: (a–c) depict OCT images of normal mucosa, epithelial hyperplasia (LEH), and oral squamous cell carcinoma (OSCC), respectively. (d–f) show the corresponding activation maps highlighting distinct feature aggregations. [2]

Advantages of Integrating OCT and AI

1. Early Detection: AI can detect subtle changes in OCT scans that may be overlooked by human observers, enabling early identification of diseases or abnormalities.

2. Improved Accuracy: AI algorithms can analyse OCT images with exceptional precision and accuracy.

3. Speed and Efficiency: AI processes OCT images much faster than humans, leading to quicker diagnosis and treatment decisions.

4. Quantitative Analysis: AI enables quantitative analyses of OCT data, providing precise measurements crucial for monitoring disease progression, treatment efficacy, and research purposes.

5. Accessibility: AI's widespread adoption can extend advanced diagnostic capabilities to regions with limited access to specialized healthcare professionals.

6. Enhanced Research Capabilities: Combining OCT and AI accelerates medical research by providing large datasets for studying diseases, drug responses, and treatment outcomes, potentially leading to significant breakthroughs. [2, 7, 11]

Limitations of Integrating OCT and AI

Challenges include the potential deskilling of physicians due to increased reliance on automation, AI's limitation in holistic clinical decision-making, the necessity for robust datasets to train AI models, and difficulties in accommodating the inherent ambiguity and variability of clinical medicine. Overcoming these obstacles requires standardizing data labeling, validating automated interpretations, and developing supportive infrastructures. Furthermore, supplying OCT imaging data for AI algorithms necessitates additional research. [2, 7]

3 | CONCLUSION

AI demonstrates promising diagnostic performance with high sensitivity in oral cancer detection. Continued advancements in image acquisition technology and AI algorithms are expected to further enhance diagnostic accuracy. AI algorithms have shown encouraging results in interpreting OCT images of oral mucosa, distinguishing between normal epithelium and precancerous or cancerous lesions. While integrating OCT and AI into clinical practice may take time, ongoing developments in AI for OCT image interpretation pave the way towards automated oral cancer screening using OCT.

CONFLICT OF INTEREST

The Authors declare no conflict of interest.

References:

1. Reddy RS, Sai Praveen KN. Optical coherence tomography in oral cancer: A transpiring domain. J Cancer Res Ther. 2017;13(6):883–8.
2. Yang Z, Pan H, Shang J, Zhang J, Liang Y. Deep-learning-based automated identification and visualization of oral cancer in optical coherence tomography images. Biomedicines. 2023;11(3).
3. Xu M, Chen Z, Zheng J, Zhao Q, Yuan Z. Artificial intelligence-aided optical imaging for cancer theranostics. Semin Cancer Biol.2023;94:62–80.
4. PODOLEANU A.G. Optical coherence tomography. Journal of Microscopy.2012; 247(3): 209-219
5. Tsai M-T, Lee H-C, Lee C-K, Yu C-H, Chen H-M, Chiang C-P, et al. Effective indicators for diagnosis of oral cancer using optical coherence tomography. Opt Express. 2008;16(20):15847–62.
6. Lee DK. Application of artificial intelligence in oral cavity cancer: A review. J Clin Otolaryngol Head Neck Surg . 2023;34(2):23–6.
7. Ramezani K, Tofangchiha M. Oral cancer screening by artificial intelligence-oriented interpretation of optical coherence tomography images. Radiol Res Pract. 2022;2022:1614838.
8. Hsieh Y-S, Ho Y-C, Lee S-Y, Chuang C-C, Tsai J-C, Lin K-F, et al. Dental optical coherence tomography. Sensors . 2013;13(7):8928–49.
9. Albrecht M, Schnabel C, Mueller J, Golde J, Koch E, Walther J. In vivo endoscopic optical coherence tomography of the healthy human oral mucosa: Qualitative and quantitative image analysis. Diagnostics. 2020;10(10):827
10. Yang Z ,Shang J, Liu C and Zhang J, Hou F ,Liang Y. Intraoperative imaging of oral-maxillofacial lesions using optical coherence tomography Journal of Innovative Optical Health Sciences.2020;13(02)
11. Hwang D-K, Chou Y-B, Lin T-C, Yang H-Y, Kao Z-K, Kao C-L, et al. Optical coherence tomography–based diabetic macula edema screening with artificial intelligence. J Chin Med Assoc . 2020;83(11):1034–8.
12. Pande P, Shrestha S, Park J, Serafino MJ, Gimenez-Conti I, Brandon J, et al. Automated classification of optical coherence tomography images for the diagnosis of oral malignancy in the hamster cheek pouch. J Biomed Opt.2014;19(8).
13. James BL, Sunny SP, Heidari AE, Ramanjinappa RD, Lam T, Tran AV, et al. Validation of a point-of-care optical coherence tomography device with machine learning algorithm for detection of oral potentially malignant and malignant lesions. Cancers.2021;13(14):3583
14. Yuan W, Yang J, Yin B, Fan X, Yang J, Sun H et al. Noninvasive Diagnosis of Oral Squamous Cell Carcinoma by Multilevel Deep Residual Learning on Optical Coherence Tomography Images. Oral diseases 2022;29(1)

How to Cite this Article: Darshana SN, Anjani SM, Ramnarayan BK, Mahesh DR, Preeti Patil.Revolutionizing oral cancer detection: Fusing the power of light and AI for early diagnosis. *W J Dent Excell. 2025; 1(1): 59-64.*